14-3-3 Protein Masks the Nuclear Localization Sequence and Blocks the Dimerization Interface of Caspase-2

Dana Kalabova[1], František Filandr[2,3], Tomas Obsil[1,4] and Veronika Obsilova[1]

[1] Dept. of Structural Biology of Signaling Proteins, Division BIOCEV, Institute of Physiology of the Czech Academy of Sciences, Vestec, Czech Republic
[2]BioCeV – Institute of Microbiology of the Czech Academy of Sciences, Vestec, Czech Republic
[3]Department of Biochemistry, Faculty of Science, Charles University in Prague, Czech Republic
[4] Dept. of Physical and Macromolecular Chemistry, Faculty of Science, Charles University in Prague, Czech Republic

Apoptosis is crucial in the maintenance of cellular homeostasis and the removal of damaged cells. Members of the caspase family of proteases play essential roles in its initiation and execution. Incorrect regulation of caspases and subsequently an apoptosis underlies the pathogenesis of many human diseases including a cancer. Many existing therapies for cancer aim to overcome apoptosis evasion by targeting different caspase pathways. It can be done indirectly by small molecules that repress natural inhibitors of caspases already present in the cell or by strategies based on directly targeting caspases. For such approaches the detailed knowledge of caspase regulation is essential. The initiator caspase-2 (C2) is activated through dimerization and autoproteolytic cleavage and inhibited through phosphorylation at Ser139 and Ser164, within the linker between the caspase recruitment and p19 domains of the zymogen, followed by association with the adaptor protein 14-3-3, which maintains C2 in its immature procaspase form (proC2).

Schematic model of regulation of caspase-2 by 14-3-3 protein

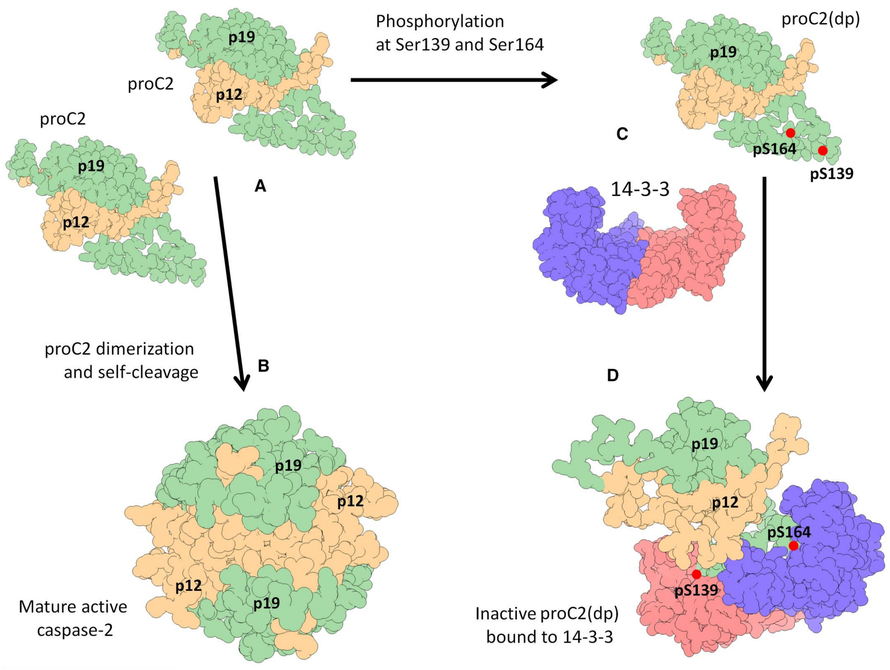

(A) Caspase-2 is activated by proximity-induced dimerization and autoproteolysis, **(B)** which generates the fully mature caspase-2 composed of two p19 and two p12 domains (colored in green and yellow, respectively). **(C)** Caspase-2 activation is controlled through phosphorylation, which triggers proC2 binding to the scaffolding dimeric 14-3-3 protein. Human proC2 contains two 14-3-3 binding motifs (pSer^{139} and pSer^{164}), located in the linker between the CARD and p19 domains, bordering the nuclear localization sequence (NLS). **(D)** The 14-3-3 protein interacts with and masks both the NLS and the C-terminal region of the p12 domain of proC2 through transient interactions. This figure was prepared using the chimerax program.

Mapping of the interactions between proC2(dp) and 14-3-3γ using HDX-MS

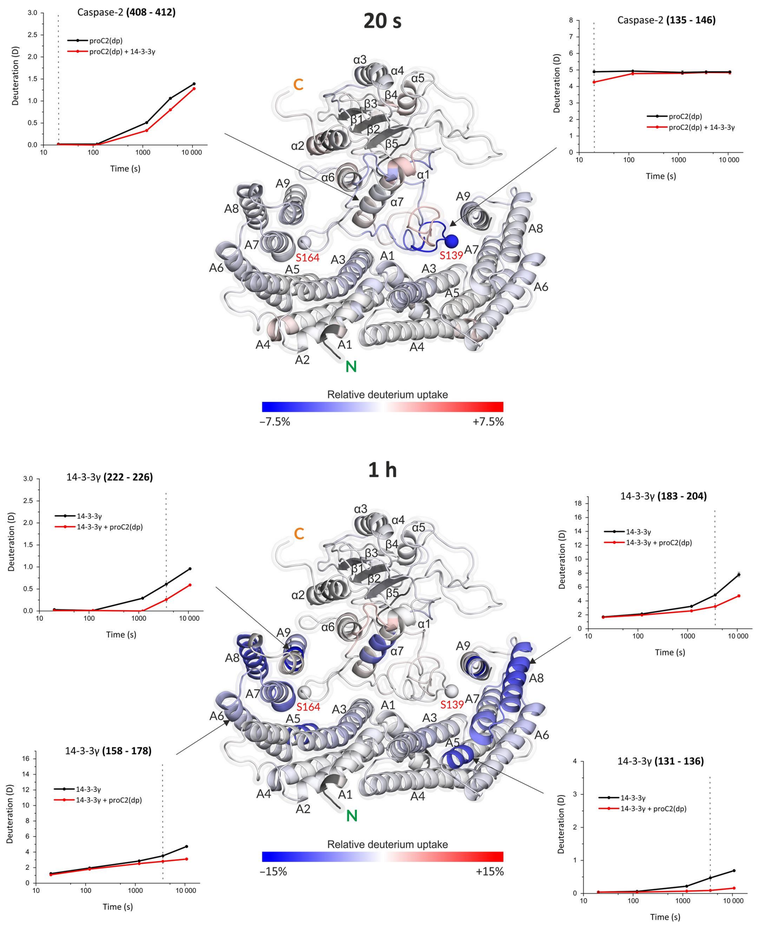

HDX-MS reveals the binding interface of proC2(dp) and 14-3-3γWT. Model of the 14-3-3γ:proC2(dp) complex with mapped changes in deuteration kinetics after complex formation shown for two deuteration times, 20 s and 1 h. Graphs representing HDX kinetics for two selected proC2(dp) regions with slower deuterium exchange kinetics upon 14-3-3γ binding are shown in the top (peptides 135–146 and 408–412). Deuterium exchange is expressed as percentage of the maximum theoretical deuteration level of proC2(dp) alone (black circles) and in the presence of 14-3-3γ (red circles). HDX kinetics for four representative 14-3-3γ peptides (131–136, 158–178, 183–204, and 222–226) are shown in the bottom. Deuterium exchange is expressed as percentage of the maximum theoretical deuteration level of 14-3-3γ alone (black circles) and in the presence of proC2(dp) (red circles). The time units are seconds. Dashed lines in the graphs represent the position in the model indicated by the arrow. Phosphorylation sites on proC2(dp) are shown as spheres. Results are the mean ± SD, *n* = 2. Structure figures were generated using PYMOL.

Crystal structure of the 14-3-3:proC2 pS139+pS164 complex

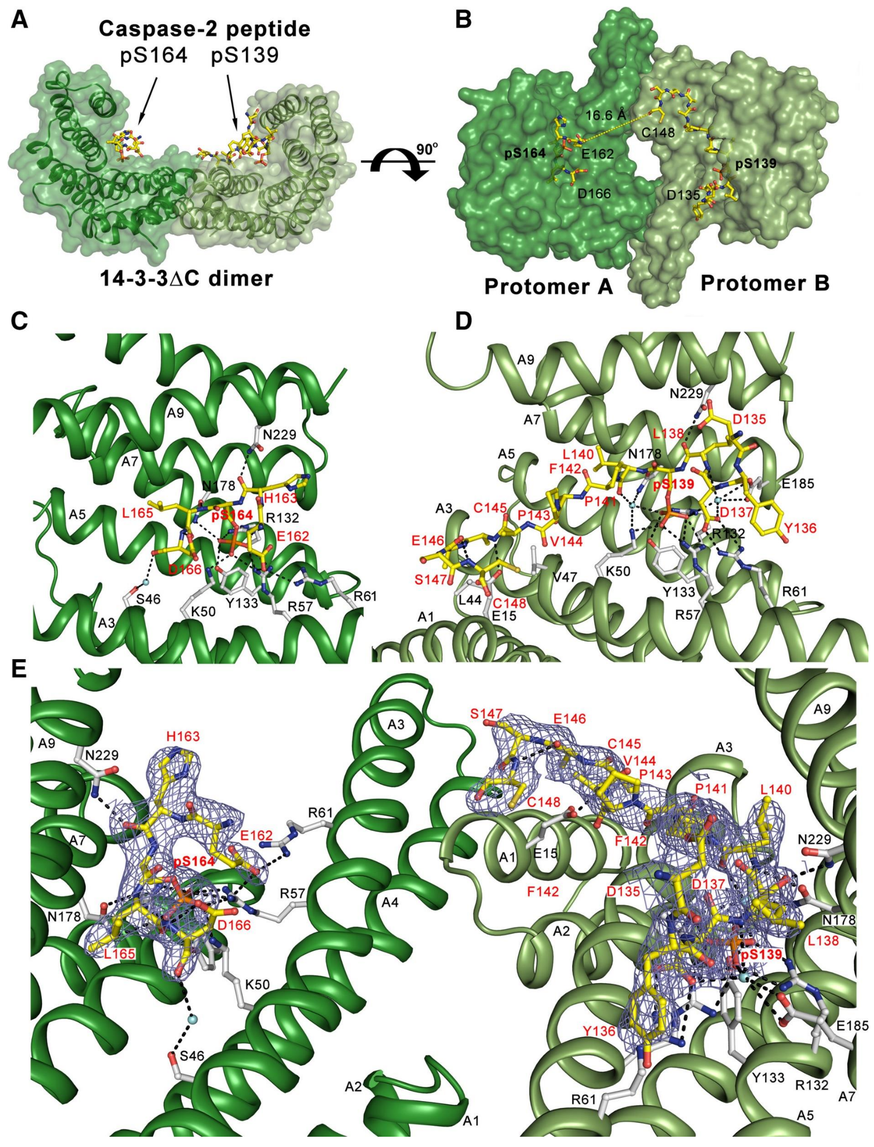

Crystal structure of the caspase-2 peptide pS139+pS164 bound to the 14-3-3γΔC dimer. (A) One asymmetric unit of the 14-3-3γΔC:pS139+pS164 crystal (PDB: 6SAD) composed of the 14-3-3γΔC dimer with bound phosphopeptide containing both pSer^{139} and pSer^{164}. 14-3-3 protomers are shown in green, as a semitransparent surface, and the phosphopeptide is shown in yellow. **(B)** Top view of the pSer^{139} and pSer^{164} sites (yellow sticks) bound to the 14-3-3 ligand-binding grooves (green surface). The dashed yellow line shows the intervening linker sequence, not visible in the crystal structure, connecting the two binding sites. **(C, D)** Contacts between 14-3-3 protomer A and B (green cartoon) containing the caspase-2 14-3-3 binding motifs pSer^{164} (A) or pSer^{139} (B) (yellow sticks). The caspase-2 residues are labeled in red, the 14-3-3 residues are labeled in black, and water molecules are shown as cyan spheres. **(E)** Top view of the intervening linker sequence of the two 14-3-3-binding motifs of caspase-2 and of the polar contacts (black dashed lines). The final $2F_o - F_c$ electron density map is contoured at 0.7σ (blue mesh). Caspase-2 residues are labeled in red, and 14-3-3 residues are labeled in black. Structure figures were generated using PYMOL.

Conclusions

The mapping of the binding interface between proC2 and 14-3-3 protein shows that 14-3-3 protein binding masks both the nuclear localization sequence (NLS), bordered by phosphorylation sites Ser139 and Ser164, and the region of the p12 domain of proC2 through transient interactions in which the p19 and p12 domains of proC2 are not firmly docked onto the surface of 14-3-3 dimer. The formation of the complex between 14-3-3 protein and proC2 does not induce any large conformational change in proC2.

14-3-3 protein masked the region of p12 domain involved in C2 activation by dimerization. Therefore, 14-3-3 protein likely inhibits proC2 activation by blocking its dimerization surface. Also, 14-3-3 protein buries the NLS of proC2, which may play an additional role in regulation of C2 activation.

References

Smidova A, Alblova M, Kalabova D, Psenakova K, Rosulek M, Herman P, Obsil T, Obsilova V. (2018) *FEBS J.* 285(22): 4196-4213.

Kalabova D, Filandr F, Alblova M, Petrvalska O, Horvath M, Man P, Obsil T, Obsilova V (2020) *FEBS J.* 287: 3494-3510.

Acknowledgement

This study was funded by the Czech Science Foundation (VO, grant number 17-00726S), the Czech Academy of Sciences (RVO:67985823 of the Institute of Physiology), project BIOCEV (CZ.1.05/1.1.00.02.0109 and LQ1604) and MEYS CR (LM2015043 CIISB, Biocev, Biophysical methods, Structural Mass Spectrometry).